

Overdamped Lattice Dynamics of Sedimenting Active Cosserat Crystals

A. Bolitho^{1,*} and R. Adhikari^{1,†}

¹*DAMTP, Centre for Mathematical Sciences, University of Cambridge, Cambridge CB3 0WA, United Kingdom*

Micropolar active matter requires for its kinematic description both positional and orientational degrees of freedom. Activity generates dynamic coupling between these kinematic variables that are absent in micropolar passive matter, such as the oriented crystals first studied by the Cosserat brothers. Here we study the effect of uniaxial activity on the dynamics of an initially crystalline state of spheroidal colloids sedimenting slowly in a viscous fluid remote from confining boundaries. Despite frictional overdamping by the fluid, the crystalline lattice admits traveling waves of position and orientation. At long wavelengths these obey a vector wave equation with Lamé constants determined by the activity. We find that at least one polarization mode of these waves is always unstable, leading to the melting of the crystal. These results are elucidated by identifying an odd-dimensional Poisson structure consisting of a Hamiltonian and an associated Casimir invariant, where linear combinations of position and orientation are identified as conjugate variables. Our results suggest that Poisson structures may exist generally for active particles in slow viscous flow and thereby allow equilibrium arguments to be applied in the presence of these dissipative systems.

I. INTRODUCTION

The continuum mechanics of crystals comprised of oriented particles was first studied theoretically by the Cosserat brothers in their monograph of 1909 [1], “*Theorie des corps déformables*”. After an initial period of neglect, this engendered the thriving field of micropolar and micromorphic continuum mechanics, where the elementary material constituent is conceived of having both a position and an orientation [2–4]. The requirement of invariance of the power expended under a rigid motion necessarily couples the position and orientation degrees of freedom and leads to a variety of macroscopic effects that have been confirmed experimentally [4–7].

Active matter [8], exemplified by suspensions of active particles in a viscous fluid [9], provides a novel example of a mechanical system where both position and orientation are relevant variables due to the breaking of microscopic rotation symmetry [10, 11]. In contrast to the Cosserat solid, however, active suspensions are comprised of two components: the particles and the solvent. In the limit where the hydrodynamics of the solvent are well modeled by the Stokes equations of slow viscous flow, the particle motion is frictionally overdamped and particle inertia plays no role in dynamical evolution. This is unlike classical Cosserat dynamics where dissipative effects are usually ignored. In addition, active forces and torques with no equilibrium analogue drive the translational and rotational behavior of these particles. Not only are these forces and torques dependent on both position and orientation, but also inject power into the surrounding solvent and thereby may be non-reciprocal and irreversible [12]. By contrast, only potential interactions are admitted in classical Cosserat dynamics which are both reciprocal and conservative. Finally, the theoretical

description of suspensions are most naturally described in the particle picture, involving coordinates and orientations, whereas classical Cosserat dynamics is formulated in the continuum picture, in terms of displacement and orientation fields.

In this paper, we study a suspension of active particles conceived as an active Cosserat crystal, comparing and contrasting their behavior with that of a Cosserat continuum. We present a theory for the overdamped mechanics of a suspension of spheroidal active particles, treating the exchange of momentum between particles and solvent consistently [13] while also respecting the group-valued character of the orientational equations of motion. Primacy is given to the kinematic equations that evolve the positions and orientations of each particle in the suspension, which may be interpreted as the action of a group on an n -fold product of Euclidean space. The generators of this action, the velocity and angular velocity, are obtained by balancing forces and torques in the absence of inertia. A virtual power principle [6, 7, 12, 14] is used to categorize the forces and torques as either conservative, dissipative or active. We obtain linearized equations of motion for the kinematic evolution with a Jacobian matrix that is determined by the derivative of the generators with respect to position and orientation. Using this general linearized kinematic equation, we study the stability of an initially crystalline arrangement of active spheroidal particles sedimenting under gravity remote from boundaries [15–19]. We find that one or more of the linear modes are always unstable which leads to the melting of the active crystal. This result is elucidated by identifying a Poisson structure within the odd-dimensional configuration manifold, consisting of a Hamiltonian in addition to conserved quantities known as Casimir invariants, with coupled orientation-sedimentation modes playing the role of conjugate momentum to lattice vibrations [20–23]. In this way, we explicitly construct Poisson brackets which completely determine dynamical evolution [24, 25]. While this form of Hamilton’s equations is not symmetric under time reversal, reflecting

* ab2075@cam.ac.uk

† ra413@cam.ac.uk

the presence of irreversible forces and torques, the non-equilibrium potential implied by the Hamiltonian admits a conceptual simplification of the stability criteria derived directly from the linear equations of motion. We conclude with a discussion on how the long-ranged stability of the active Cosserat crystal differs from that of the active Cosserat medium and how this approach may be generally useful in overdamped active particle mechanics [26–34].

II. OVERDAMPED ACTIVE MECHANICS

We consider $i = 1, \dots, N$ uniaxial rigid particles of mass m and moment of inertia tensor \mathcal{I} whose centers of mass are located at \mathbf{R}_i and whose orientations are specified by the unit vector \mathbf{p}_i . The kinematic configuration space is the N -fold direct product of three-dimensional Euclidean space \mathbb{E}^3 (the space of positions) and the two-sphere S^2 (the space of orientations). The velocities \mathbf{V}_i and angular velocities $\boldsymbol{\Omega}_i$ determine the evolution on this configuration manifold through the kinematic equations,

$$\dot{\mathbf{R}}_i = \mathbf{V}_i, \quad \dot{\mathbf{p}}_i = \boldsymbol{\Omega}_i \times \mathbf{p}_i. \quad (1)$$

The velocities and angular velocities are themselves determined by Newton's equations of motion for linear and angular momentum, [13, 34]

$$m\dot{\mathbf{V}}_i = \mathbf{F}_i, \quad \mathcal{I} \cdot \dot{\boldsymbol{\Omega}}_i + \boldsymbol{\Omega}_i \times \mathcal{I} \cdot \boldsymbol{\Omega}_i = \mathbf{T}_i \quad (2)$$

where \mathbf{F}_i and \mathbf{T}_i are the total force and torque acting on the i -th particle. It is convenient to classify the forces and torques by their contribution to the balance of energy. To this end, we introduce the kinetic energy of the system through the positive-definite quadratic form

$$K = \frac{1}{2}m\mathbf{V}_i \cdot \mathbf{V}_i + \frac{1}{2}\boldsymbol{\Omega}_i \cdot \mathcal{I} \cdot \boldsymbol{\Omega}_i \quad (3)$$

where repeated particle indices are summed over. Multiplying the equation for linear momentum by \mathbf{V}_i , the equation of angular momentum by $\boldsymbol{\Omega}_i$, and summing over all particles we obtain an equation relating the rate of change of kinetic energy to the power expended by the forces and torques,

$$\frac{dK}{dt} = \mathbf{F}_i \cdot \mathbf{V}_i + \mathbf{T}_i \cdot \boldsymbol{\Omega}_i. \quad (4)$$

Conservative forces and torques are defined to be even under time reversal and for which the power expended is the total derivative:

$$\mathbf{F}_i^C \cdot \mathbf{V}_i + \mathbf{T}_i^C \cdot \boldsymbol{\Omega}_i = -\frac{dU}{dt}. \quad (5)$$

This implies the existence of a multibody potential energy function $U = U(\mathbf{R}_1, \dots, \mathbf{R}_N, \mathbf{p}_1, \dots, \mathbf{p}_N)$ of the positions and orientations which is even under time reversal. Consistency with the time derivative of this function and the kinematic equations then implies that the conservative forces and torques are related to the potential as

$$\mathbf{F}_i^C = -\frac{\partial U}{\partial \mathbf{R}_i}, \quad \mathbf{T}_i^C = -\mathbf{p}_i \times \frac{\partial U}{\partial \mathbf{p}_i}. \quad (6)$$

Here we confine our attention to mechanical systems in which the dissipative forces and torques are linear functions of the velocities and angular velocities

$$\begin{aligned} \mathbf{F}_i^D &= -(\gamma_{ij}^{TT} \mathbf{V}_j + \gamma_{ij}^{TR} \boldsymbol{\Omega}_j) = \frac{\partial \mathcal{R}}{\partial \mathbf{V}_i}, \\ \mathbf{T}_i^D &= -(\gamma_{ji}^{RT} \mathbf{V}_j + \gamma_{ij}^{RR} \boldsymbol{\Omega}_j) = \frac{\partial \mathcal{R}}{\partial \boldsymbol{\Omega}_i}. \end{aligned} \quad (7)$$

Power dissipation is then a positive-definite quadratic form of the velocities and angular velocities determined by the Rayleigh dissipation function

$$\gamma_{ij}^{TT} \mathbf{V}_i \mathbf{V}_j + 2\gamma_{ij}^{TR} \mathbf{V}_i \boldsymbol{\Omega}_j + \gamma_{ij}^{RT} \boldsymbol{\Omega}_i \boldsymbol{\Omega}_j = 2\mathcal{R} > 0. \quad (8)$$

The matrices γ_{ij}^{TT} , γ_{ij}^{TR} , γ_{ij}^{RR} are symmetric and positive-definite friction tensors which determine the dissipative forces and torques. These, in general, are many-body functions of the positions and orientations of each particle. For a particle with three planes of symmetry, the resistance tensors obey the constraint [11]

$$\gamma_{ij}^{TR} = \gamma_{ij}^{RT}, \quad \gamma_{ii}^{TR} = \gamma_{ii}^{RT} = 0 \quad (9)$$

where no sum is implied on the repeated i index. Considering the remainder of the forces and torques in Eq.(4) to be non-conservative, odd under time reversal and power injecting leads to the following energy balance equation:

$$\frac{d}{dt}(K + U) = -2\mathcal{R} + \mathbf{F}_i^A \cdot \mathbf{V}_i + \mathbf{T}_i^A \cdot \boldsymbol{\Omega}_i. \quad (10)$$

This identification of the active forces, \mathbf{F}_i^A , and active torques, \mathbf{T}_i^A , is similar to the definition proposed by Finlayson and Scriven, where active Cauchy stresses in fluid mechanical continua are identified through a power principle [12].

When the rate of change of kinetic energy is negligible in the power balance, the dynamics become overdamped and the rate of change of potential energy is balanced by dissipation and active power injection. In this limit, the velocities and angular velocities can be obtained directly from the simultaneous solution of the momentum and angular momentum balance equations,

$$\begin{aligned} \mathbf{V}_i &= \boldsymbol{\mu}_{ij}^{TT} \cdot (\mathbf{F}_j^C + \mathbf{F}_j^A) + \boldsymbol{\mu}_{ij}^{TR} \cdot (\mathbf{T}_j^C + \mathbf{T}_j^A), \\ \boldsymbol{\Omega}_i &= \boldsymbol{\mu}_{ij}^{RT} \cdot (\mathbf{F}_j^C + \mathbf{F}_j^A) + \boldsymbol{\mu}_{ij}^{RR} \cdot (\mathbf{T}_j^C + \mathbf{T}_j^A). \end{aligned} \quad (11)$$

The mobility tensors $\boldsymbol{\mu}_{ij}^{TT}, \boldsymbol{\mu}_{ij}^{TR}, \boldsymbol{\mu}_{ij}^{RR}$ are inverse to the friction tensors introduced above and therefore inherit identical symmetry properties. The kinematic equations are closed by the above relations and provide the time-evolution of the overdamped mechanical system.

For a passive mechanical system ($\mathbf{F}_i^A = 0, \mathbf{T}_i^A = 0$) in unbounded potentials, it remains possible that dissipation is balanced by loss in potential energy resulting in a dynamical steady state. However, for a potential bounded from below, a dynamical fixed point is reached with zero velocity and angular velocity, and vanishing conservative forces and torques. In contrast, for an active mechanical system ($\mathbf{F}_i^A \neq 0, \mathbf{T}_i^A \neq 0$), even in the presence of a potential bounded from below, a dynamical steady state can be reached where the rate of change of potential energy is balanced by dissipation and the active injection of power. These steady states could either be fixed points or limit cycles of the overdamped dynamical system. Much of the surprising aspects of active mechanical systems can be traced to this property, as will be apparent in what follows.

III. LINEARIZED KINEMATICS

We now consider active particles with initial configuration ($\mathbf{R}_i^*, \mathbf{p}_i^*$) where \mathbf{R}_i^* is a lattice vector and \mathbf{p}_i^* is a constant vector. Perturbations about this state take the form

$$\mathbf{R}_i = \mathbf{R}_i^* + \mathbf{u}_i, \quad \mathbf{p}_i = \mathbf{p}_i^* + \mathbf{q}_i. \quad (12)$$

Expanding the velocity and angular velocity to first order in these perturbations yields

$$\begin{aligned} \mathbf{V}_i &= \mathbf{V}_i^* + \left[\frac{\partial \mathbf{V}_i}{\partial \mathbf{R}_j} \right]_* \cdot \mathbf{u}_j + \left[\frac{\partial \mathbf{V}_i}{\partial \mathbf{p}_j} \right]_* \cdot \mathbf{q}_j, \\ \boldsymbol{\Omega}_i &= \boldsymbol{\Omega}_i^* + \left[\frac{\partial \boldsymbol{\Omega}_i}{\partial \mathbf{R}_j} \right]_* \cdot \mathbf{u}_j + \left[\frac{\partial \boldsymbol{\Omega}_i}{\partial \mathbf{p}_j} \right]_* \cdot \mathbf{q}_j. \end{aligned} \quad (13)$$

Inserting this into Eq.(1) yields

$$\begin{aligned} \dot{\mathbf{u}}_i &= \mathbf{V}_i^* + \left[\frac{\partial \mathbf{V}_i}{\partial \mathbf{R}_j} \right]_* \cdot \mathbf{u}_j + \left[\frac{\partial \mathbf{V}_i}{\partial \mathbf{p}_j} \right]_* \cdot \mathbf{q}_j, \\ \dot{\mathbf{q}}_i &= \boldsymbol{\Omega}_i^* \times \mathbf{p}_i^* + \left[\mathbf{p}_i \times \frac{\partial \boldsymbol{\Omega}_i}{\partial \mathbf{R}_j} \right]_* \cdot \mathbf{u}_j \\ &\quad + \boldsymbol{\Omega}_i^* \times \mathbf{q}_i + \left[\mathbf{p}_i \times \frac{\partial \boldsymbol{\Omega}_i}{\partial \mathbf{p}_j} \right]_* \cdot \mathbf{q}_j, \end{aligned} \quad (14)$$

where the zeroth order terms $\mathbf{V}_i^*, \boldsymbol{\Omega}_i^* \times \mathbf{p}_i^*$ represent rigid body motions of the initial state. When $\boldsymbol{\Omega}_i^* \times \mathbf{p}_i^* = 0$ and the \mathbf{V}_i^* are the same for every particle, we may transform to a co-moving frame where the dynamics are defined by a $6N \times 6N$ linear system of $3N$ translational and $3N$ rotational degrees of freedom

$$\frac{d}{dt} \begin{pmatrix} \mathbf{u}_i \\ \mathbf{q}_i \end{pmatrix} = \begin{pmatrix} \mathbf{J}^{uu} & \mathbf{J}^{uq} \\ \mathbf{J}^{qu} & \mathbf{J}^{qq} \end{pmatrix}_{ij} \begin{pmatrix} \mathbf{u}_j \\ \mathbf{q}_j \end{pmatrix} \quad (15)$$

which describes the linear evolution of perturbations with $3N \times 3N$ block Jacobian matrices taking the form

$$\begin{aligned} \mathbf{J}_{ij}^{uu} &= \frac{\partial \mathbf{V}_i}{\partial \mathbf{R}_j}, & \mathbf{J}_{ij}^{uq} &= \frac{\partial \mathbf{V}_i}{\partial \mathbf{p}_j}, \\ \mathbf{J}_{ij}^{qu} &= \mathbf{p}_i^* \times \frac{\partial \boldsymbol{\Omega}_i}{\partial \mathbf{R}_j}, & \mathbf{J}_{ij}^{qq} &= \mathbf{p}_i^* \times \frac{\partial \boldsymbol{\Omega}_i}{\partial \mathbf{p}_j}. \end{aligned} \quad (16)$$

For the overdamped dynamics, these Jacobian matrices can be obtained from the differentials of the velocities and angular velocities

$$\begin{aligned} d\mathbf{V}_i &= d\boldsymbol{\mu}_{ij}^{TT} \cdot (\mathbf{F}_j^C + \mathbf{F}_j^A) + d\boldsymbol{\mu}_{ij}^{TR} \cdot (\mathbf{T}_j^C + \mathbf{T}_j^A) \\ &\quad + \boldsymbol{\mu}_{ij}^{TT} \cdot d(\mathbf{F}_j^C + \mathbf{F}_j^A) + \boldsymbol{\mu}_{ij}^{TR} \cdot d(\mathbf{T}_j^C + \mathbf{T}_j^A), \\ d\boldsymbol{\Omega}_i &= d\boldsymbol{\mu}_{ij}^{RT} \cdot (\mathbf{F}_j^C + \mathbf{F}_j^A) + d\boldsymbol{\mu}_{ij}^{RR} \cdot (\mathbf{T}_j^C + \mathbf{T}_j^A) \\ &\quad + \boldsymbol{\mu}_{ij}^{RT} \cdot d(\mathbf{F}_j^C + \mathbf{F}_j^A) + \boldsymbol{\mu}_{ij}^{RR} \cdot d(\mathbf{T}_j^C + \mathbf{T}_j^A). \end{aligned} \quad (17)$$

These differentials receive contributions from the infinitesimal changes in the mobilities and the infinitesimal changes in the forces and torques as the configurations $\mathbf{R}_i, \mathbf{p}_i$ are varied. It is important to note that the differentials of the configurations must obey the N kinematic constraints $\mathbf{p}_i \cdot \dot{\mathbf{p}}_i = \mathbf{p}_i \cdot (\boldsymbol{\Omega}_i \times \mathbf{p}_i) = 0$. This reflects the fact that \mathbf{p}_i is a coordinate on S^2 requiring $\mathbf{p}_i^* \cdot \mathbf{q}_i = 0$. Orientational fluctuations are therefore described by the remaining two degrees of freedom in \mathbf{q}_i . In particular, the differential $d\mathbf{p}$ must be perpendicular to \mathbf{p}_i^* and thus for a parametrization $\mathbf{p}_i^* = (0, 0, 1)$ this implies $d\mathbf{p} = (dp_x, dp_y, 0)$. In the following section we specify the forms of the mobilities and the forces and torques for a suspension of hydrodynamically interacting active particles.

IV. ACTIVE FORCES AND TORQUES

The most common experimental realization of an overdamped active mechanical system, in the sense of Sec. (II), is a suspension of active colloids [35–40]. Active colloids are endowed with microscopic mechanisms that generate slip velocities on the particle-fluid boundaries. An expansion of the slip that yields self-propulsion and self-rotation takes the form [13]

$$\mathbf{v}_i^A = \mathbf{V}_i^A + \boldsymbol{\Omega}_i^A \times \boldsymbol{\rho}_i \quad (18)$$

where $\boldsymbol{\rho}_i$ is a vector parameterizing the surface of the i -th particle. The coefficients \mathbf{V}_i^A and $\boldsymbol{\Omega}_i^A$ are here taken to be functions of the orientation of the i -th particle and will be specified below. The slips produces stresses in the fluid that act back on the particles as tractions on the particle-fluid boundaries. The active forces and torques are obtained by integrating

$$\mathbf{F}_i^A = \int \mathbf{t}_i^A dS_i, \quad \mathbf{T}_i^A = \int \boldsymbol{\rho}_i \times \mathbf{t}_i^A dS_i \quad (19)$$

where \mathbf{t}_i^A is the slip-dependent traction on the i -th particle due to its own activity and that of all the remaining particles. The linearity of the Stokes equations and of the boundary conditions implies that the active forces and torques are of the form [13, 41]

$$\begin{aligned}\mathbf{F}_i^A &= \gamma_{ij}^{TT} \cdot \mathbf{V}_j^A + \gamma_{ij}^{TR} \cdot \boldsymbol{\Omega}_j^A, \\ \mathbf{T}_i^A &= \gamma_{ij}^{RT} \cdot \mathbf{V}_j^A + \gamma_{ij}^{RR} \cdot \boldsymbol{\Omega}_j^A\end{aligned}\quad (20)$$

which represent a generalization of Stokes laws of friction for active colloids. This specifies the velocities and angular velocities of the particles in terms of their configuration in a manner that is consistent with the conservation of momentum and angular momentum in the suspension.

The hydrodynamic self-mobilities for a body with uniaxial spheroidal symmetry must be of the form [11, 42]

$$\begin{aligned}\mu_{ii}^{TT} &= \mu_1^T (\mathbf{I} - \mathbf{p}_i \mathbf{p}_i) + \mu_2^T \mathbf{p}_i \mathbf{p}_i, \\ \mu_{ii}^{RR} &= \mu_1^R (\mathbf{I} - \mathbf{p}_i \mathbf{p}_i) + \mu_2^R \mathbf{p}_i \mathbf{p}_i, \\ \mu_{ii}^{TR} &= \mu_{ii}^{RT} = 0\end{aligned}\quad (21)$$

where no summation is implied on the i index. The scalar coefficients $\mu_1^T \neq \mu_2^T$ and $\mu_1^R \neq \mu_2^R$ reflect the anisotropy of the translational and rotational responses along and perpendicular to the axis of uniaxial symmetry. There is no hydrodynamic coupling between translation and rotation in the absence of chirality, as we have noted before in Eq.(9). The mutual mobilities in the pair approximation are given by

$$\begin{aligned}\mu_{ij}^{TT} &= \mathcal{F}_i^0(\mathbf{p}_i) \mathcal{F}_j^0(\mathbf{p}_j) \mathbf{G}_{ij}(\mathbf{R}_i, \mathbf{R}_j), \\ \mu_{ij}^{RT} &= \frac{1}{2} \mathcal{F}_i^1(\mathbf{p}_i) \mathcal{F}_j^0(\mathbf{p}_j) \nabla_{\mathbf{R}_i} \times \mathbf{G}_{ij}(\mathbf{R}_i, \mathbf{R}_j),\end{aligned}\quad (22)$$

where \mathbf{G}_{ij} is a Green's function of the Stokes equation that determines the bulk fluid flow resulting from a point force, while \mathcal{F}_i^0 and \mathcal{F}_i^1 are Faxén operators that correct for the finite size of the particles [42, 43]. In the dilute limit, the leading contributions to the mutual mobilities do not depend on the finiteness of the particles and the Faxén operators may be set to the identity. The Green's function for a linear medium of infinite extent is given by

$$\mathbf{G}(\mathbf{R}_i, \mathbf{R}_j) = A_1 \mathbf{I} + A_2 \hat{\mathbf{r}}_{ij} \hat{\mathbf{r}}_{ij}, \quad (23)$$

where $\mathbf{r}_{ij} = \mathbf{R}_i - \mathbf{R}_j$ and $\hat{\mathbf{r}}_{ij} = \mathbf{r}_{ij}/r_{ij}$ is the normalized separation between particles i and j . For a viscous overdamped Stokes medium, the Oseen tensor is defined with the coefficients

$$A_1 = A_2 = \frac{1}{8\pi\eta r_{ij}}, \quad (24)$$

where η is the viscosity of the external fluid. Specific choices of the active velocities and angular velocities $\mathbf{V}_A, \boldsymbol{\Omega}_A$ along with conservative forces and torques $\mathbf{F}^C, \mathbf{T}^C$ can now be made to study particular overdamped active systems.

V. SEDIMENTING ACTIVE CRYSTALS

We now investigate the linear stability of a lattice of identical active particles sedimenting under gravity in a Stokesian fluid of infinite extent. This idealizes relevant experiment conditions [15, 16, 19] where active particles remain remote from the boundaries of the container. The conservative and active forces are determined by the expressions

$$\begin{aligned}\mathbf{F}_i^C &= m\mathbf{g}, \quad \mathbf{T}_i^C = 0, \\ \mathbf{V}_i^A &= v_A \mathbf{p}_i, \quad \boldsymbol{\Omega}_i^A = \omega_A \mathbf{p}_i,\end{aligned}\quad (25)$$

where m is the buoyant mass of the particle, v_A is the active speed and ω_A is the active angular speed. The rigid body motion of the particles is then determined by the pair of equations

$$\begin{aligned}\mathbf{V}_i &= \sum_j \mu_{ij}^{TT} \cdot m\mathbf{g} + v_A \mathbf{p}_i, \\ \boldsymbol{\Omega}_i &= \sum_{j \neq i} \mu_{ij}^{RT} \cdot m\mathbf{g} + \omega_A \mathbf{p}_i,\end{aligned}\quad (26)$$

representing the one-body translational motion of the i -th particle under gravitational force and active motion, and hydrodynamic two-body interactions due to entrainment in the flow field produced by the other sedimenting particles. The rotational motion of the i -th particle has no one-body hydrodynamic contribution and reorientation results entirely from the vorticity produced by the sedimentation flow. These equations generalize the dynamics of active particle pairs presented in [34] to a many-body system. The elements of the Jacobian matrix that follow from the above are

$$\begin{aligned}\mathbf{J}_{ij}^{uu} &= \sum_l \left[\frac{\partial \mu_{il}^{TT}}{\partial \mathbf{R}_j} \cdot m\mathbf{g} \right]_*, \\ \mathbf{J}_{ij}^{uq} &= \sum_l \left[\frac{\partial \mu_{il}^{TT}}{\partial \mathbf{p}_j} \cdot m\mathbf{g} \right]_* + v_A \delta_{ij} \text{diag}(1, 1, 0), \\ \mathbf{J}_{ij}^{qu} &= \sum_l \left[\mathbf{p}_i \times \frac{\partial \mu_{il}^{RT}}{\partial \mathbf{R}_j} \cdot m\mathbf{g} \right]_*, \\ \mathbf{J}_{ij}^{qq} &= 0.\end{aligned}\quad (27)$$

In the following sections we shall use these to analyze the stability of one- and two-dimensional lattice.

We conclude this section with an observation about the contributions from geometric anisotropy and activity to translational motion. Combining Eqs.(21,26), the velocity of the i -th particle may be expressed as

$$\mathbf{V}_i = \mu_1^T m\mathbf{g} - [(\mu_1^T - \mu_2^T)(\mathbf{p}_i \cdot m\mathbf{g}) - v_A] \mathbf{p}_i + \text{HI} \quad (28)$$

where the contributions to the one-body mobility from geometric anisotropy and activity have been made clear and where HI includes mutual hydrodynamic contributions. Here, geometric anisotropy adds an apolar term

to the velocity while activity adds a polar term. For small perturbation, however, the contribution takes the form

$$\mathbf{J}_{ii}^{uq} \cdot \mathbf{q}_i = [(\mu_1^T - \mu_2^T) mg + v_A] \mathbf{q}_i \quad (29)$$

showing that it is not possible to distinguish geometric anisotropy from activity at the level of the linearized equations of motion. We may therefore define an effective active speed

$$\tilde{v} = (\mu_1^T - \mu_2^T) mg + v_A \quad (30)$$

encapsulating both the passive effect of geometric anisotropy and the active effect of self-propulsion as the single relevant parameter controlling the dynamics. In what follows, we shall assume spherical particles of radius b with $\mu_1^T = \mu_2^T = \mu^T = 6\pi\eta b$ with a self-propulsion speed v_A , with the understanding that this causes no loss of generality.

VI. ONE-DIMENSIONAL LATTICE

We now consider a one-dimensional lattice of particles with initial positions and orientations

$$\mathbf{R}_i^* = (x_i^*, 0, 0), \quad \mathbf{p}_i^* = (0, 0, 1) \quad (31)$$

where $x_i^* = ia$ and a is the lattice spacing. The discrete translational invariance of the system can be exploited to diagonalize the linearized dynamics in terms of plane wave collective modes

$$\mathbf{u}_i(t) = b \int \frac{dk}{2\pi} e^{ikx_i^*} \mathbf{u}_k(t), \quad \mathbf{q}_i(t) = \int \frac{dk}{2\pi} e^{ikx_i^*} \mathbf{q}_k(t),$$

where the wave vector $\mathbf{k} = (k, 0, 0)$ is directed along the chain. Inserting these plane wave solutions into Eq.(15) and summing over all lattice points yields the Fourier-transformed linear equations of motion

$$\frac{d}{dt} \begin{pmatrix} \mathbf{u}_k \\ \mathbf{q}_k \end{pmatrix} = \begin{pmatrix} \mathbf{J}^{uu} & \mathbf{J}^{uq} \\ \mathbf{J}^{qu} & \mathbf{J}^{qq} \end{pmatrix}_k \begin{pmatrix} \mathbf{u}_k \\ \mathbf{q}_k \end{pmatrix}, \quad (32)$$

where the block Jacobian elements are given by

$$\mathbf{J}_k^{\alpha\beta} = \sum_{\text{lattice}} \mathbf{J}_{ij}^{\alpha\beta} e^{-ik(x_i^* - x_j^*)}.$$

with $\alpha, \beta \in \{u, q\}$. A schematic of the initial condition and kinematic variables is presented in Fig.(1). Introducing the Stokes velocity v_0 , the Stokes time τ and the dimensionless active speed v through the relations

$$v_0 = \mu^T mg, \quad \tau = b/v_0, \quad v = \tilde{v}/v_0$$

and evaluating the required matrix elements (detailed in Appendix A), the Jacobian matrix in the plane-wave basis is

$$\mathbf{J}_k = \left(\begin{array}{ccc|ccc} 0 & 0 & -s(k) & v & 0 & 0 \\ 0 & 0 & 0 & 0 & v & 0 \\ s(k) & 0 & 0 & 0 & 0 & 0 \\ \hline -2c(k) & 0 & 0 & 0 & 0 & 0 \\ 0 & c(k) & 0 & 0 & 0 & 0 \\ 0 & 0 & 0 & 0 & 0 & 0 \end{array} \right), \quad (33)$$

where

$$\begin{aligned} \lambda &= \frac{3b^2}{2a}, \\ s(k) &= \frac{i\lambda}{a} \sum_{n=1}^{\infty} \frac{\sin(nka)}{n^2} \equiv s, \\ c(k) &= \frac{\lambda b}{a^2} \sum_{n=1}^{\infty} \frac{\cos(nka) - 1}{n^3} \equiv c. \end{aligned} \quad (34)$$

We note that $s(k)$ is purely imaginary while $c(k)$ is real and negative. The collective modes consist of a longitudinal positional polarization u_{1k} , a pair of transverse positional polarizations u_{2k}, u_{3k} , a longitudinal orientational polarization q_{1k} and a transverse orientational polarization q_{2k} . The constraint $\mathbf{p}^* \cdot \mathbf{q}_k$ eliminates the third degree of freedom in the orientational collective mode \mathbf{q}_k so that only five degrees of freedom remain. This is represented by the vanishing of the final row and column in \mathbf{J}_k leading to a trivial null eigenvalue. The remaining dynamical degrees of freedom yield five non-trivial linear equations of motion

$$\begin{aligned} \dot{u}_{1k} &= -su_{3k} + vq_{1k}, & \dot{u}_{2k} &= vq_{2k}, & \dot{u}_{3k} &= su_{1k}, \\ \dot{q}_{1k} &= -2cu_{1k}, & \dot{q}_{2k} &= cu_{2k}. \end{aligned} \quad (35)$$

These equations show that the couplings between the positional and orientational collective modes are not symmetric, a property that can be traced to the non-potential character of the active forces and torques. The linear system decouples into two subspaces. The first subspace consists of the triplet u_{1k}, q_{1k}, u_{3k} which are a pair of longitudinal modes and the transverse mode parallel to gravity. These obey the linear equations

$$\frac{d}{dt} \begin{pmatrix} u_{1k} \\ q_{1k} \\ u_{3k} \end{pmatrix} = \begin{pmatrix} 0 & v & -s \\ -2c & 0 & 0 \\ s & 0 & 0 \end{pmatrix} \begin{pmatrix} u_{1k} \\ q_{1k} \\ u_{3k} \end{pmatrix}. \quad (36)$$

One may construct a conserved quantity orthogonal to the dynamical flow given by

$$\mathcal{E}_0 = 2cu_{3k} + sq_{1k} \equiv r_k, \quad \dot{r}_k = 0.$$

This non-trivial conserved quantity reflects the fact that local activity may work to oppose passive clumping of the

lattice. The dimensionality of the first subspace is therefore reduced by one, leading to the appearance of two linearly independent position-orientation-sedimentation coupled eigenmodes given by

$$\mathcal{E}_{1\pm} = \pm \sqrt{-s^2 - 2cvu_{1k} + vq_{1k} - su_{3k}}. \quad (37)$$

The positive sign denotes an in-phase longitudinal position and orientation wave while the negative sign denotes its anti-phase counterpart. These eigenmodes obey the harmonic equation

$$\ddot{\mathcal{E}}_{1\pm} = -\omega_1^2 \mathcal{E}_{1\pm}, \quad \omega_1^2 = s^2 + 2cv. \quad (38)$$

This immediately implies the existence of stable harmonic waves of frequency ω_1 when $v < -s^2/2c$, which is negative, such that $\omega_1^2 > 0$ [19]. Conversely, when $v > -s^2/2c$ the square of the frequency $\omega_1^2 < 0$ leads to the presence of an exponentially growing mode \mathcal{E}_{1+} while the conjugate mode \mathcal{E}_{1-} is exponentially decaying. The solution for passive spheres is obtained by taking $v = 0$ which immediately implies that passive sedimenting one-dimensional lattices are unstable [15]. The second subspace consists of the pair of transverse modes u_{2k}, q_{2k} which obey the linear equations

$$\frac{d}{dt} \begin{pmatrix} u_{2k} \\ q_{2k} \end{pmatrix} = \begin{pmatrix} 0 & v \\ c & 0 \end{pmatrix} \begin{pmatrix} u_{2k} \\ q_{2k} \end{pmatrix}. \quad (39)$$

This leads to the appearance of two linearly independent transverse position-orientation coupled eigenmodes given by

$$\mathcal{E}_{2\pm} = \pm \sqrt{cvu_{2k} + vq_{2k}}. \quad (40)$$

Again, the positive sign denotes an in-phase transverse position and orientation wave while the negative sign denotes its anti-phase counterpart. These eigenmodes obey a different harmonic equation given by

$$\ddot{\mathcal{E}}_{2\pm} = -\omega_2^2 \mathcal{E}_{2\pm}, \quad \omega_2^2 = -cv. \quad (41)$$

In this case, for $v > 0$ we obtain wavelike solutions of frequency ω_2 . However, for $v < 0$ we see that the square of the frequency $\omega_2^2 < 0$ leads to the presence of an exponentially growing mode \mathcal{E}_{2+} while the conjugate mode \mathcal{E}_{2-} is exponentially decaying. For passive spheres, $v = \omega_2 = 0$ such that transverse perturbations are neither stable nor unstable. Together, we see that there is no value of v for which both longitudinal and transverse modes are stable, and thus an exponentially growing solution will always be present. Furthermore, for the range of parameter values $0 > v > -s^2/2c$ both transverse and longitudinal modes $\mathcal{E}_{1+}, \mathcal{E}_{2+}$ are unstable.

In the following section we show that these equations of motion admit symplectic structure. This allows us to reformulate the stability criteria through the construction of a scalar Hamiltonian function, thus elucidating the stability mechanism of the crystal.

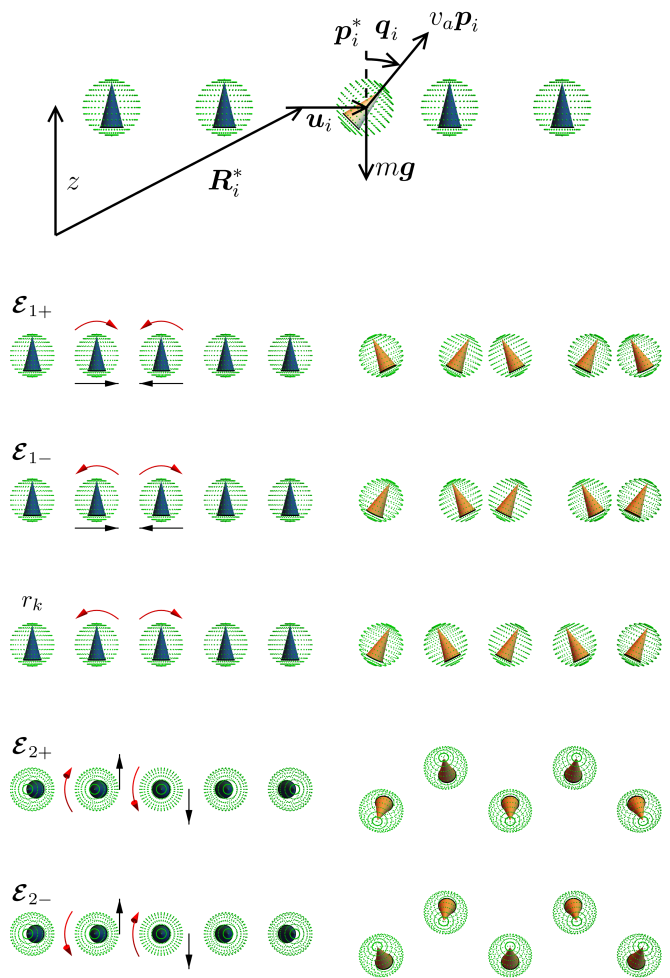


Figure 1. The first panel shows a schematic of the sedimenting one-dimensional crystal as specified by Eqs.(14,31). The remaining panels present a graphical depiction of the collective modes presented in Tab.(I) evaluated at wavenumber $k = \pi/2$. The first three modes lie in the space co-ordinatized by the triplet (u_{1k}, q_{1k}, u_{3k}) and are viewed perpendicular to the direction of gravity while the remaining two modes lie in the space co-ordinatized by the pair (u_{2k}, q_{2k}) and are viewed along the direction of gravity.

A. Poisson structure

We start by making the co-ordinate transformations

$$p_{1k} = -su_{3k} + vq_{1k}, \quad p_{2k} = vq_{2k} \quad (42)$$

such that the linear evolution can be cast in the form

$$\frac{d}{dt} \begin{pmatrix} u_{1k} \\ u_{2k} \\ p_{1k} \\ p_{2k} \\ r_k \end{pmatrix} = \begin{pmatrix} 0 & 0 & 1 & 0 & 0 \\ 0 & 0 & 0 & 1 & 0 \\ -1 & 0 & 0 & 0 & 0 \\ 0 & -1 & 0 & 0 & 0 \\ 0 & 0 & 0 & 0 & 0 \end{pmatrix} \nabla H_k, \quad (43)$$

Eigenvalue Λ_α	Eigenvector \mathcal{E}_α	Interpretation
$\Lambda_0 = 0$	$r_k = 2cu_{3k} + sq_{1k}$	one-body orientation coupled to sedimentation velocity
$\Lambda_{1\pm} = \pm\omega_1$	$\mathcal{E}_{1\pm} = \pm\sqrt{-s^2 - 2cvu_{1k} + vq_{1k} - su_{3k}}$	coupled in-/anti-phase longitudinal position-orientation mode
$\Lambda_{2\pm} = \pm\omega_2$	$\mathcal{E}_{2\pm} = \pm\sqrt{cvu_{2k} + vq_{2k}}$	coupled in-/anti-phase transverse position-orientation mode

Table I. Tabulation of the eigensystem of Eq.(33) where $\omega_1^2 = s^2 + 2cv$, $\omega_2^2 = -cv$.

$$\nabla = \left(\partial/\partial u_{1k}, \partial/\partial u_{2k}, \partial/\partial p_{1k}, \partial/\partial p_{2k}, \partial/\partial r_k \right),$$

with Hamiltonian

$$H_k = \frac{1}{2} (p_{1k}^2 + p_{2k}^2) + \frac{1}{2} (\omega_1^2 u_{1k}^2 + \omega_2^2 u_{2k}^2), \quad (44)$$

where p_{1k}, p_{2k} are momentum-like variables conjugate to longitudinal and transverse displacements respectively. p_{1k} consists of a linear combination of orientation and position co-ordinates, while p_{2k} is purely orientational. Dynamical evolution is therefore completely determined by this Hamiltonian, preserving the symplectic form $dp_1 \wedge du_1 + dp_2 \wedge du_2$, and yielding a conserved quantity r_k known as a Casimir function [20–23]. The reduction of the state-space to a direct product of a symplectic manifold and Casimir functions is known as Poisson dynamics, generalizing Hamiltonian dynamics to odd-dimensional manifolds. The equations of motion then take the form

$$\dot{q}_{ak} = \{q_{ak}, H_k\}, \quad \dot{p}_{ak} = \{p_{ak}, H_k\}$$

where $a \in \{1, 2\}$ and the Poisson bracket is given by

$$\{A_k, H_k\} = \frac{\partial A_k}{\partial q_{ak}} \frac{\partial H_k}{\partial p_{ak}} - \frac{\partial H_k}{\partial q_{ak}} \frac{\partial A_k}{\partial p_{ak}}.$$

We now use this Hamiltonian to elucidate the stability behavior of the Poisson orbits. The potential function

$$U_k = \frac{1}{2} (\omega_1^2 u_{1k}^2 + \omega_2^2 u_{2k}^2) \quad (45)$$

may either be a saddle or parabolic, depending on the signs of ω_1^2 and ω_2^2 . For $v > 0$ we already deduced that $\omega_1^2 < 0$ while $\omega_2^2 > 0$ characterizing a saddle with unstable direction aligned along u_{1k} . For $0 > v > -s^2/2c$ both $\omega_1^2, \omega_2^2 < 0$ resulting in an unstable parabolic potential. If v is decreased further, $\omega_1 > 0$ defining a saddle with unstable direction aligned along u_{2k} . Contour plots of U_k as v is varied are presented in Fig.(2a). Fig.(2b) depicts a plot of the Hessian function which shows that the potential only becomes parabolic in the range $0 > v > -s^2/2c$.

While the sedimenting lattice is always unstable for sedimenting active spheres, we may consider an anisotropic body, or an active colloid where the activity depends on spatial direction with longitudinal and transverse components v_1, v_2 , yielding a modified dispersion relation

$$\omega_1^2 = s^2 + 2cv_1, \quad \omega_2^2 = -cv_2. \quad (46)$$

Now the potential may become positive-definite if v_1, v_2 contain opposite signatures, resulting in the appearance

of stable bound orbits with frequencies ω_1, ω_2 in the longitudinal and transverse directions respectively (see Fig.(2c-d)). These frequencies are almost certainly non-commensurate and hence indicate quasi-periodicity of the orbits. Such a situation may be realized experimentally by considering a one-dimensional chain of sedimenting triaxial bodies with minor axis aligned longitudinally and major axis aligned transverse to the chain, or through imposition of external fields in the transverse and longitudinal directions. In the next section, we develop an equivalent continuum Cosserat theory that models an active filament and compare this to the lattice-based theory.

B. Continuum approximation

We now derive approximate equations of motion for the dynamics of an active Cosserat filament, the continuum analogue of the active Cosserat chain. Here, displacement and orientation variables are now functions of an additional continuous variable x parameterizing the filament in addition to time. As the lattice length scale $a \rightarrow 0$, we utilize the long-wavelength form of the dispersion relations to construct our continuum theory. However, taking the long-wavelength limit directly in Eq.(34) leads to divergent lattice sums, since both s, c are non-analytic in their gradients at $k = 0$ due to the long-ranged hydrodynamic forces present. We therefore truncate these sums to $n = 1$, corresponding to considering hydrodynamic effects from nearest neighbors alone, while discarding long-ranged effects. This yields analytic approximations

$$\begin{aligned} s(k) &\equiv s = i \frac{\lambda}{a} \sin ka \approx i\lambda k, \\ c(k) &\equiv c = \frac{\lambda b}{a^2} (\cos ka - 1) \approx -\frac{1}{2} \lambda b k^2. \end{aligned} \quad (47)$$

The dispersion relations are then

$$\begin{aligned} \omega_1^2 &= s^2 + 2cv \approx -\lambda(\lambda + vb)k^2, \\ \omega_2^2 &= -cv \approx \frac{1}{2} \lambda v b k^2. \end{aligned} \quad (48)$$

In analogy with Eq.(35), the continuum equations that produce this dispersion are given by

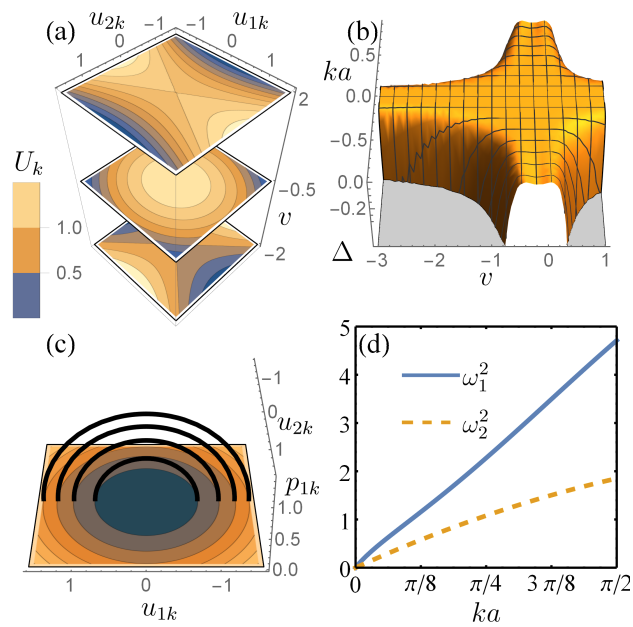


Figure 2. (a) Contour plots of the potential U_k for $v = -2, -0.5, 2$. For $v = 2$ the u_{1k} direction is stable while the u_{2k} direction is unstable. For $v = -0.5$ both u_{1k} and u_{2k} directions are unstable. For $v = -2$ the u_{1k} direction is unstable while the u_{2k} direction is stable. (b) Plot of the Hessian determinant $\Delta = \omega_1^2 \omega_2^2$ of U_k against v, ka . Negative values of Δ indicate the presence of a saddle point with a single unstable mode, while positive values of Δ indicate a parabolic potential with two unstable modes since $\Delta > 0$ when $0 > v > -s^2/2c$. (c) Contour plot of Eq.(45) for anisotropic activity $v_1 = -1.5, v_2 = 1$ with a superimposed Poincaré recurrence plot at $u_{2k} = 0$. The appearance of closed one-dimensional contours indicates stable quasiperiodic orbital behavior. (d) Plot of ω_1^2, ω_2^2 against ka for the same anisotropic activity. These frequencies are positive for all values of ka leading to a stable positive definite Hamiltonian with massless dispersion.

$$\begin{aligned} \dot{u}_1 &= -\lambda \frac{\partial u_3}{\partial x} + vbq_1, & \dot{u}_2 &= vbq_2, & \dot{u}_3 &= \lambda \frac{\partial u_1}{\partial x}, \\ \dot{q}_1 &= -\lambda \frac{\partial^2 u_1}{\partial x^2}, & \dot{q}_2 &= \frac{1}{2} \lambda \frac{\partial^2 u_2}{\partial x^2}. \end{aligned} \quad (49)$$

These dynamics contain the conserved function

$$\frac{\partial r}{\partial t} = \frac{\partial}{\partial t} \left(\lambda \frac{\partial^2 u_3}{\partial x^2} + \lambda \frac{\partial q_1}{\partial x} \right) = 0$$

while the remaining variables close yielding the second order equations.

$$\frac{\partial^2 u_1}{\partial t^2} = -\lambda(\lambda + vb) \frac{\partial^2 u_1}{\partial x^2}, \quad \frac{\partial^2 u_2}{\partial t^2} = \frac{1}{2} \lambda vb \frac{\partial^2 u_2}{\partial x^2}. \quad (50)$$

These equations also contain Poisson structure defined by the Hamiltonian density

$$\mathcal{H} = \frac{1}{2} (\pi_1^2 + \pi_2^2) + \frac{1}{2} \left[\alpha \left(\frac{\partial u_1}{\partial x} \right)^2 + \beta \left(\frac{\partial u_2}{\partial x} \right)^2 \right], \quad (51)$$

where

$$\alpha = -\lambda(\lambda + vb), \quad \beta = \frac{1}{2} \lambda vb \quad (52)$$

and now

$$\pi_1 = \partial_t u_1, \quad \pi_2 = \partial_t u_2. \quad (53)$$

Eqs.(50,53) together are then equivalent to the set of first order equations given by

$$\dot{\boldsymbol{\pi}}(x) = \{\boldsymbol{\pi}(x), H\}, \quad \dot{\mathbf{u}}(x) = \{\mathbf{u}(x), H\}, \quad (54)$$

where the Hamiltonian $H = \int \mathcal{H}(x) dx$ and we have defined Poisson brackets

$$\{\mathcal{A}(x), H\} = \int \frac{\delta \mathcal{A}(x)}{\delta \mathbf{u}(x')} \frac{\delta H}{\delta \boldsymbol{\pi}(x')} - \frac{\delta H}{\delta \mathbf{u}(x')} \frac{\delta \mathcal{A}(x)}{\delta \boldsymbol{\pi}(x')} dx'.$$

On the one hand, by performing a gradient expansion only keeping a finite number of terms of the lattice sum, the resulting instability is of a similar form to that studied by Crowley [15]. On the other hand, the dispersion relation derived by considering the full hydrodynamics of an infinite sedimenting lattice is non-analytic, resulting in the formation of a cusp as $k \rightarrow 0$ (see Fig.(3)). As a consequence, the continuum theory is unable to reproduce the behavior of the lattice-based model at zero wavenumber. Instabilities of this type were first studied by Felderhof [44]. In addition, for certain values of v the dispersion relation derived from the full lattice dynamics predicts a long-wavelength instability that is absent from the dispersion relations of the approximate continuum theory, as shown in Fig.(3b). Unlike the Felderhof instability, this discrepancy results from the truncation of the analytic function performed in Eq.(48) and its effects may be included in the field theory by redefining the lattice parameters to include a functional dependence on k of the form

$$\begin{aligned} \alpha(k) &= \omega_1^2(k)/k^2, \\ \beta(k) &= \omega_2^2(k)/k^2, \end{aligned} \quad (55)$$

where ω_1, ω_2 depend on the bare lengthscales λ, b . In this way, we see that it is possible to formulate a continuum theory of the active Cosserat filament that reproduces the dispersion behavior of the lattice-based model for $k \neq 0$. This procedure is reminiscent of a renormalization process whereby that the lattice parameters depend on the lengthscale at which a system is probed.

VII. TWO DIMENSIONAL LATTICE

We now consider an infinite sedimenting two-dimensional lattice with initial positions and orientations

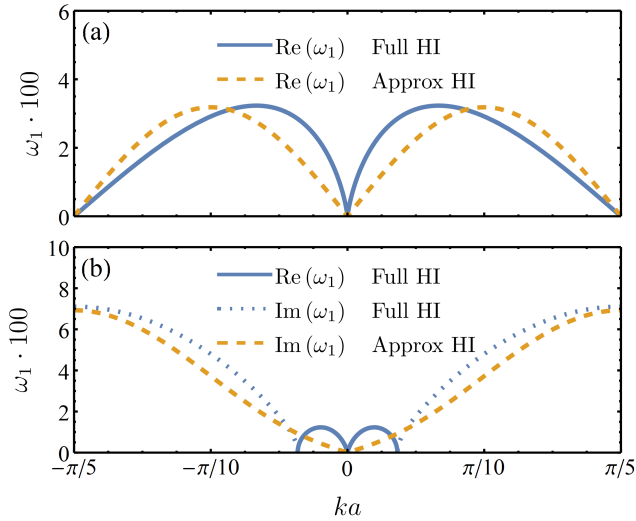


Figure 3. Comparison of instabilities in one-dimension through plots of ω_1 . (a) Here, $v = 0$ corresponding to passive sedimenting spheres with entirely real and positive dispersion relations. When long-ranged hydrodynamics are taken into account, the dispersion relation forms a non-analytic cusp around $k = 0$. For $k > 0$ the two dispersion relations qualitatively predict a similar lattice instability (b) Here, $v = -1/20$ and the dispersion relations no longer qualitatively agree at finite wavelength. The inclusion of long-ranged hydrodynamics leads to a discrepancy between the approximate dispersion relation, which is purely imaginary, and the full dispersion relation which contains real and imaginary contributions. Therefore, erroneous conclusions about the lattice stability may be drawn from the bare continuum field theory, where lattice parameters are not allowed to run with lengthscale.

$$\mathbf{R}_i^* = (x_i^*, y_i^*, 0), \quad \mathbf{p}_i^* = (0, 0, 1) \quad (56)$$

where x_i^*, y_i^* define the initial lattice configuration. The plane wave collective modes

$$\mathbf{u}_i(t) = b \int \frac{d^2k}{4\pi^2} e^{i(k_1 x_i^* + k_2 y_i^*)} \mathbf{u}_k(t),$$

$$\mathbf{q}_i(t) = \int \frac{d^2k}{4\pi^2} e^{i(k_1 x_i^* + k_2 y_i^*)} \mathbf{q}_k(t),$$

where $\mathbf{k} = (k_1, k_2, 0)$ may be inserted into Eq.(15) to yield lattice dynamics with explicit form

$$\mathbf{J}_k = \left(\begin{array}{ccc|ccc} 0 & 0 & -s\hat{k}_1 & v & 0 & 0 \\ 0 & 0 & -s\hat{k}_2 & 0 & v & 0 \\ s\hat{k}_1 & s\hat{k}_2 & 0 & 0 & 0 & 0 \\ \hline c(1 - 3\hat{k}_1\hat{k}_1) & -3c\hat{k}_1\hat{k}_2 & 0 & 0 & 0 & 0 \\ -3c\hat{k}_1\hat{k}_2 & c(1 - 3\hat{k}_2\hat{k}_2) & 0 & 0 & 0 & 0 \\ 0 & 0 & 0 & 0 & 0 & 0 \end{array} \right) \quad (57)$$

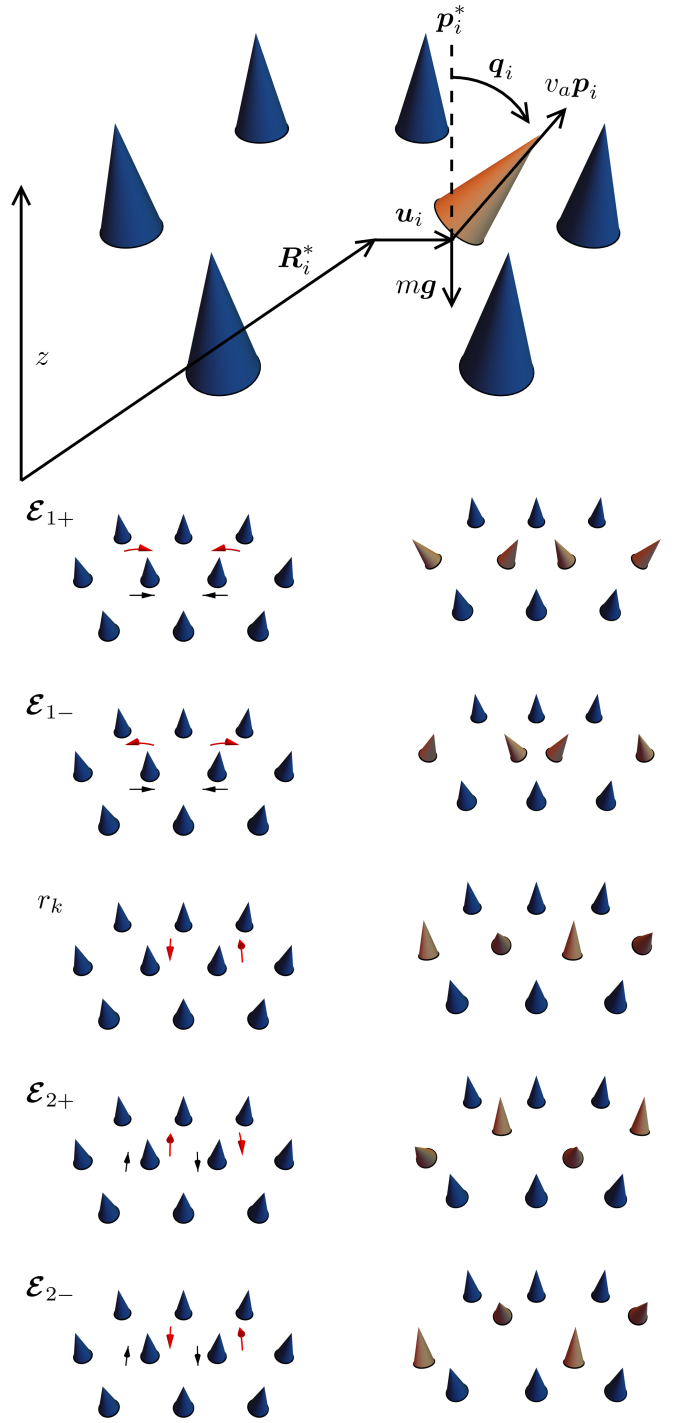


Figure 4. The first panel shows a schematic of the sedimenting two-dimensional crystal as specified by Eqs.(14,56). The remaining panels present a graphical depiction of the collective modes evaluated at wavenumber $k = \pi/2$. The first three modes lie in the space co-ordinatized by the triplet $(u_{\parallel k}, q_{\parallel k}, u_{3k})$ while the remaining two modes lie in the space co-ordinatized by the pair $(u_{\perp k}, q_{\perp k})$.

where we define $\hat{k}_1 = k_1/k$, $\hat{k}_2 = k_2/k$. The lattice sums $s(\mathbf{k}) \equiv s$, $c(\mathbf{k}) \equiv c$ are defined in Appendix B. Once again, s is purely imaginary while c is real and negative. The collective modes now consist of positional polarizations $\tilde{\mathbf{u}}_k, u_{3k}$ and orientational polarizations \mathbf{q}_k where

$$\tilde{\mathbf{u}}_k = (u_{1k}, u_{2k}, 0) \quad (58)$$

are the components of \mathbf{u}_k in the xy plane, u_{3k} is the component of \mathbf{u}_k resolved parallel to gravity and $\mathbf{q}_k = \tilde{\mathbf{q}}_k$ is a vector in the xy plane due to the constraint $\mathbf{p}^* \cdot \mathbf{q}_k = 0$. In this way, both $\tilde{\mathbf{u}}_k, \tilde{\mathbf{q}}_k$ are vectors in the plane perpendicular to gravity and the final row and column of \mathbf{J}_k vanish leading to the presence of a trivial null eigenvalue. The remaining dynamical degrees of freedom yield the five non-trivial linear equations of motion

$$\begin{aligned} \dot{\tilde{\mathbf{u}}}_k &= -s\hat{k}u_{3k} + v\mathbf{q}_k, & \dot{u}_{3k} &= s\hat{k} \cdot \tilde{\mathbf{u}}_k, \\ \dot{\mathbf{q}}_k &= c(\mathbf{I} - 3\hat{k}\hat{k}) \cdot \tilde{\mathbf{u}}_k. \end{aligned} \quad (59)$$

Again, non-symmetric coupling between positional and orientational collective modes is indicative of the non-potential character of the active forces and torques and this linear system decouples into two subspaces. The first subspace consists of positional and orientational modes longitudinal to \hat{k} given by

$$u_{\parallel k} = \hat{k}\hat{k} \cdot \mathbf{u}_k, \quad q_{\parallel k} = \hat{k}\hat{k} \cdot \mathbf{q}_k, \quad (60)$$

respectively, in addition to the transverse mode u_{3k} parallel to gravity. These obey the linear equations

$$\frac{d}{dt} \begin{pmatrix} u_{\parallel k} \\ q_{\parallel k} \\ u_{3k} \end{pmatrix} = \begin{pmatrix} 0 & v & -s \\ -2c & 0 & 0 \\ s & 0 & 0 \end{pmatrix} \begin{pmatrix} u_{\parallel k} \\ q_{\parallel k} \\ u_{3k} \end{pmatrix}. \quad (61)$$

While this equation looks identical to Eq.(36), the values for s, c are different from those in Sec.(VI) as the lattice sum is now over a two-dimensional crystal. However, as this form is similar to that in Sec.(VI) we may repeat our analysis, deducing a conserved quantity orthogonal to the dynamical flow given by

$$\mathcal{E}_0 = 2cu_{3k} + sq_{\parallel k} \equiv r_k, \quad \dot{r}_k = 0. \quad (62)$$

This non-trivial conserved quantity again reflects the fact that local activity can work to oppose passive clumping of the lattice [16]. The dimensionality of the first subspace is therefore reduced by one and is hence spanned by a pair of eigenmodes

$$\mathcal{E}_{\parallel\pm} = \pm\sqrt{-s^2 - 2cv}u_{\parallel k} + vq_{\parallel k} - su_{3k}. \quad (63)$$

The positive sign denotes an in-phase position and orientation wave directed along \hat{k} while the negative sign denotes its anti-phase counterpart. These eigenmodes obey the harmonic equation

$$\ddot{\mathcal{E}}_{\parallel\pm} = -\omega_{\parallel}^2 \mathcal{E}_{\parallel\pm}, \quad \omega_{\parallel}^2 = s^2 + 2cv. \quad (64)$$

Again, we see the appearance of stable harmonic waves of frequency ω_{\parallel} when $v < -s^2/2c$, which is negative, such that $\omega_{\parallel}^2 > 0$. Conversely, when $v > -s^2/2c$ the square of the frequency $\omega_{\parallel}^2 < 0$ implies the presence of an exponentially growing mode $\mathcal{E}_{\parallel+}$ while the conjugate mode $\mathcal{E}_{\parallel-}$ is exponentially decaying. The solution for passive spheres is obtained by taking $v = 0$ which immediately implies that passive sedimenting two-dimensional lattices are unstable [16].

The second subspace consists of positional and orientational modes transverse to both \hat{k} and u_{3k} consisting of the linear perturbation modes $u_{\perp k} = (\mathbf{I} - \hat{k}\hat{k}) \cdot \mathbf{u}_k, q_{\perp k} = (\mathbf{I} - \hat{k}\hat{k}) \cdot \mathbf{q}_k$ which obey the equations

$$\frac{d}{dt} \begin{pmatrix} u_{\perp k} \\ q_{\perp k} \end{pmatrix} = \begin{pmatrix} 0 & v \\ c & 0 \end{pmatrix} \begin{pmatrix} u_{\perp k} \\ q_{\perp k} \end{pmatrix}. \quad (65)$$

This leads to the appearance of two linearly independent transverse position-orientation coupled eigenmodes given by

$$\mathcal{E}_{\perp\pm} = \pm\sqrt{cv}u_{\perp k} + vq_{\perp k}. \quad (66)$$

Again, the positive sign denotes a transverse in-phase position and orientation wave while the negative sign denotes its anti-phase counterpart. These eigenmodes obey a different harmonic equation given by

$$\ddot{\mathcal{E}}_{\perp\pm} = -\omega_{\perp}^2 \mathcal{E}_{\perp\pm}, \quad \omega_{\perp}^2 = -cv. \quad (67)$$

In this case, it is clear that for $v > 0$ we obtain wavelike solutions of frequency ω_{\perp} . However, for $v < 0$ we see that the square of the frequency $\omega_{\perp}^2 < 0$ implying the presence of an exponentially growing mode $\mathcal{E}_{\perp+}$ while the conjugate mode $\mathcal{E}_{\perp-}$ is exponentially decaying. For passive spheres, $\omega_{\perp} = 0$ and transverse perturbations are neither stable nor unstable. Together, we see that there is no value of v for which both longitudinal and transverse modes are stable, and thus an exponentially growing solution will always be present. Furthermore, for the range of parameter values $0 > v > -s^2/2c$ both transverse and longitudinal modes $\mathcal{E}_{\parallel+}, \mathcal{E}_{\perp+}$ are unstable. Where previously the one-dimensional chain explicitly broke rotational symmetry, here the discrete rotational symmetry of the two-dimensional crystal is only broken upon the application of a wave-like perturbation with wavemode \mathbf{k} . In this way, the longitudinal and transverse directions to this wavevector provide a natural co-ordinate system, diagonalizing Eq.(57) and rendering it in the same form as Eq.(33). In the next section, we show that the two-dimensional lattice also admits symplectic structure allowing us to reformulate the stability criteria through the construction of a scalar Hamiltonian function as done previously.

A. Poisson structure

We start by making the co-ordinate transformations

$$p_{\parallel k} = -s u_{3k} + v q_{\parallel k}, \quad p_{\perp k} = v q_{\perp k} \quad (68)$$

which immediately yields the Poisson structure

$$\frac{d}{dt} \begin{pmatrix} u_{\parallel k} \\ u_{\perp k} \\ p_{\parallel k} \\ p_{\perp k} \\ r_k \end{pmatrix} = \begin{pmatrix} 0 & 0 & 1 & 0 & 0 \\ 0 & 0 & 0 & 1 & 0 \\ -1 & 0 & 0 & 0 & 0 \\ 0 & -1 & 0 & 0 & 0 \\ 0 & 0 & 0 & 0 & 0 \end{pmatrix} \nabla H_k, \quad (69)$$

$$\nabla = \left(\partial/\partial u_{\parallel k}, \partial/\partial u_{\perp k}, \partial/\partial p_{\parallel k}, \partial/\partial p_{\perp k}, \partial/\partial r_k \right)$$

with Hamiltonian

$$H_k = \frac{1}{2} (p_{\parallel k}^2 + p_{\perp k}^2) + \frac{1}{2} (\omega_{\parallel}^2 u_{\parallel k}^2 + \omega_{\perp}^2 u_{\perp k}^2), \quad (70)$$

where

$$\omega_{\parallel}^2 = (s^2 + 2cv) \quad \omega_{\perp}^2 = -cv. \quad (71)$$

Here, $p_{\parallel k}, p_{\perp k}$ are momentum-like variables conjugate to $u_{\parallel k}, u_{\perp k}$. $p_{\parallel k}$ consists of a linear combination of orientation and position co-ordinates, while $p_{\perp k}$ is purely orientational. Dynamical evolution is therefore completely determined by this Hamiltonian, preserving the symplectic form $dp_{\parallel} \wedge du_{\parallel} + dp_{\perp} \wedge du_{\perp}$, and yielding a conserved Casimir function r_k [20–23]. The equations of motion may then be written in the form

$$\dot{q}_{ak} = \{q_{ak}, H_k\}, \quad \dot{p}_{ak} = \{p_{ak}, H_k\}$$

where $a \in \{\parallel, \perp\}$ and the Poisson bracket is given by

$$\{A_k, H_k\} = \frac{\partial A_k}{\partial q_{ak}} \frac{\partial H_k}{\partial p_{ak}} - \frac{\partial H_k}{\partial q_{ak}} \frac{\partial A_k}{\partial p_{ak}}.$$

We now use this Hamiltonian to elucidate the stability behavior of the Poisson orbits. Once again, the potential function

$$U_k = \frac{1}{2} (\omega_{\parallel}^2 u_{\parallel k}^2 + \omega_{\perp}^2 u_{\perp k}^2) \quad (72)$$

is parabolic when $0 > v > -s^2/2c$ such that both $\omega_{\parallel}^2, \omega_{\perp}^2 < 0$ and a saddle-point for all other values of v , whereby either $\omega_{\parallel}^2 < 0$ and $\omega_{\perp}^2 > 0$ or $\omega_{\parallel}^2 > 0$ and $\omega_{\perp}^2 < 0$. We therefore see that, for isotropic activity, the lattice is unstable for all values of v . However, if the crystal is composed of particles that deform anisotropically or are polarized upon macroscopic perturbations of the crystal, the activity may decompose into unique parts v_{\parallel}, v_{\perp} transverse and perpendicular to the applied perturbation. This yields a modified dispersion relation

$$\omega_{\parallel}^2 = s^2 + 2cv_{\parallel}, \quad \omega_{\perp}^2 = -cv_{\perp}. \quad (73)$$

In this way, the potential U_k may become positive-definite for certain values of v_{\parallel} and v_{\perp} resulting in stable orbits.

B. Continuum approximation

We now derive approximate continuum equations of motion for the dynamics of the active Cosserat sheet, the continuum analogue of the two-dimensional active Cosserat crystal. Here, displacement and orientation variables are now functions of the two continuous variables x, y in addition to time. Following Sec.(VIb), the hydrodynamics are truncated to only include nearest neighbor interactions yielding

$$\begin{aligned} \mathbf{s}(\mathbf{k}) &= i \frac{\lambda}{a} (\hat{\mathbf{x}} \sin k_1 a + \hat{\mathbf{y}} \sin k_2 a) \approx i \lambda \mathbf{k}, \\ c(\mathbf{k}) &= \frac{\lambda b}{a^2} [\cos k_1 a + \cos k_2 a - 2] \approx -\frac{1}{2} \lambda b k^2. \end{aligned} \quad (74)$$

$\mathbf{s}(\mathbf{k})$ is a vectorial quantity which is proportional to the applied perturbation direction \mathbf{k} when the corresponding sum is taken over all lattice points (see Appendix B). When this sum is truncated to nearest neighbors, the underlying point group is exposed by the lattice vectors $\hat{\mathbf{x}}, \hat{\mathbf{y}}$. However, in the long-wavelength limit the crystal appears isotropic and \mathbf{s} once again can only depend on \mathbf{k} . Using Eq.(59) immediately leads to the continuum equations

$$\begin{aligned} \dot{\tilde{\mathbf{u}}} &= -\lambda \nabla u_z + v b \mathbf{q}, \quad \dot{u}_3 = \lambda \nabla \cdot \tilde{\mathbf{u}}, \\ \dot{\mathbf{q}} &= \frac{1}{2} \lambda (\nabla^2 \tilde{\mathbf{u}} - 3 \nabla \nabla \cdot \tilde{\mathbf{u}}), \end{aligned} \quad (75)$$

where $\nabla = (\partial_x, \partial_y, 0)$ denotes a gradient operator taken in the plane perpendicular to gravity. These equations contain a conserved function

$$\frac{\partial r}{\partial t} = \frac{\partial}{\partial t} (\nabla^2 u_3 + \nabla \cdot \mathbf{q}_k) = 0, \quad (76)$$

and can be closed yielding the second order evolution

$$\ddot{\tilde{\mathbf{u}}} = -\lambda \left(\lambda + \frac{3}{2} v b \right) \nabla \nabla \cdot \tilde{\mathbf{u}} + \frac{1}{2} \lambda v b \nabla^2 \tilde{\mathbf{u}}. \quad (77)$$

This equation is identical to that of a linear elastic medium where $-\lambda(\lambda + 3vb/2), \lambda vb/2$ are the Lamé parameters. However, unlike an elastic medium, the compression modulus of the active medium may be negative, resulting in further contraction and instability upon application of external pressure or shearing. We can define a Hamiltonian density

$$\mathcal{H} = \frac{1}{2} \pi^2 + \frac{1}{2} \left[\alpha (\nabla \cdot \tilde{\mathbf{u}})^2 + \beta (\nabla \tilde{\mathbf{u}})^2 \right], \quad (78)$$

where

$$\alpha = -\lambda \left(\lambda + \frac{3}{2} v b \right), \quad \beta = \frac{1}{2} \lambda v b \quad (79)$$

and now

$$\boldsymbol{\pi} = \partial_t \mathbf{u}. \quad (80)$$

Eqs.(77,80) together are then equivalent to the set of first order equations given by

$$\dot{\boldsymbol{\pi}}(\mathbf{x}) = \{H, \boldsymbol{\pi}(\mathbf{x})\}, \quad \dot{\mathbf{u}}(\mathbf{x}) = \{H, \mathbf{u}(\mathbf{x})\}. \quad (81)$$

where the Hamiltonian $H = \int \mathcal{H}(\mathbf{x}) d^2\mathbf{x}$ and we have defined Poisson brackets given by

$$\{H, \mathcal{A}(\mathbf{x})\} = \int \frac{\delta H}{\delta \mathbf{u}(\mathbf{x}')} \frac{\delta \mathcal{A}(\mathbf{x})}{\delta \boldsymbol{\pi}(\mathbf{x}')} - \frac{\delta H}{\delta \boldsymbol{\pi}(\mathbf{x}')} \frac{\delta \mathcal{A}(\mathbf{x})}{\delta \mathbf{u}(\mathbf{x}')} d^2\mathbf{x}'.$$

The Hamiltonian density is manifestly rotationally invariant with geometric factors α, β dependent on the underlying microstructure. As shown previously, stable sedimentation may only occur if activity or microscopic deformation is induced by the applied perturbation. This is similar to many microstructural materials that display microscopic anisotropy upon application of macroscopic strain or shearing. Once again, this can result in two anisotropy parameters, v_1, v_2 , along and transverse to the applied deformation which, through similar analysis as done previously, may yield stable Poisson orbits. A possible system that may exhibit this behavior is sedimenting arrays of electrically charged fluid droplets which deform under lattice compression. The dispersion relations formulated this way display a similar discrepancy compared to the full lattice-based dynamics as discussed in Sec.(VIb). This results in both the running of the lattice parameters α, β with lengthscale, which can be included in the continuum theory, and the appearance of a Felderhof instability [44] which cannot be included in the continuum theory.

VIII. DISCUSSION

On the one hand, the appearance of Poisson structure in the active Cosserat crystal may be expected, since it can be shown that any odd-dimensional linear system yields a Poisson structure [45]. On the other hand, many previous examples of non-linear symplectic structure arising in the field of active matter share a common feature, namely the identification of orientation variables as conjugate momenta to displacements [26–34]. We suspect a similar structure is present in previous works involving two-body problems and that additional Lie symmetries could be found, reducing the dynamical space to a single conjugate pair. This implies a certain non-trivial ubiquity of Poissonian dynamics within the field of active matter, even at non-linear order, which appears to be a rich area for further research. The recurrence of symplectic structure can be rationalized through the following heuristic argument: many active system share a common motif with regards to time-evolution whereby position variables are updated according to orientational state while orientation variables are updated according to positional state. The absence of an on-diagonal response, as seen in Eqs.(33,57), implies conservation of phase volume which, in two dimensions, is a conserved symplectic form. Indeed, both the one- and two-dimensional

Cosserat crystals can be decoupled into two- and three-dimensional Hamiltonian and Poissonian subsystems of the entire state-space, comprised of transverse and longitudinal dynamics respectively, whereby the conjugate momenta are monotonically dependent on orientation variables.

Furthermore, the presence of a non-analytic point at zero wavenumber in both the one- and two-dimensional active Cosserat crystals is indicative of an instability of the type studied by Felderhof [44] and results due to the presence of long-ranged hydrodynamic forces. This feature cannot be modeled well by gradient expansion methods, which amount to a nearest-neighbor approximation of the full theory [15–17], and leads to a discrepancy between continuum theories and discrete lattice-based analysis at wavenumber $k = 0$.

To conclude this section, we remark that this Poissonian interpretation of the sedimentation behavior of active Cosserat crystals can be used to understand hydrodynamically-mediated crystallization at fluid boundaries [37, 40, 46, 47]. In analogy with our previous work, [34], we expect the boundary to provide a type of forcing through hydrodynamic interactions, which may be damped by the inclusion of further external forces and torques. We defer investigation into the possible steady-state behavior to future work [48].

IX. CONCLUSION

We investigated the sedimentation behavior of both the sedimenting one- and two-dimensional active Cosserat crystal in an overdamped external medium and, using a virtual power principle [7], derive the geometrical equations of motion for the lattice of active uniaxial colloidal particles. In the presence of an overdamped external medium, inertial forces are negligible and the lattice dynamics evolve on a five-dimensional state-space of translation and orientation modes. Remarkably, this state-space is endowed with Poisson structure [20–23] even in the absence of inertial and conservative forces, with coupled sedimentation-orientation co-ordinates playing the role of conjugate momenta to the lattice displacements. We identify conserved Casimir functions and a simple harmonic Hamiltonian with activity dependent frequencies. Together, these form a symplectic foliation of the dynamical state-space, thereby reducing the problem to one of Hamiltonian dynamics. This is exploited to reveal the presence of stable position-orientation-sedimentation coupled limit-cycle behavior, which is shown to occur in both one- and two-dimensions, in the presence of anisotropic activity.

ACKNOWLEDGMENTS

We acknowledge the EPSRC (AB) and the Isaac Newton Trust (RA) for support. We thank Prof. M. E. Cates

and Prof. R. E. Goldstein for helpful discussions and

critical remarks. We thank Prof. R. E. Goldstein for bringing [14] to our attention.

-
- [1] E. Cosserat and F. Cosserat, *Theorie des corps déformables* (A. Hermann et fils, 1909).
- [2] C. Kafadar and A. C. Eringen, *International Journal of Engineering Science* **9**, 271 (1971).
- [3] A. C. Eringen, *International Journal of Engineering Science* **5**, 191 (1967).
- [4] H. Altenbach, G. A. Maugin, and V. Erofeev, *Mechanics of generalized continua*, Vol. 7 (Springer, 2011).
- [5] E. Kroner, in *Proc. IUTAM Symposium* (Springer, 1968).
- [6] P. Germain, *Mathematics and Mechanics of Complex Systems* **8**, 153 (2020).
- [7] P. Germain, *SIAM Journal on Applied Mathematics* **25**, 556 (1973).
- [8] M. C. Marchetti, J. F. Joanny, S. Ramaswamy, T. B. Liverpool, J. Prost, M. Rao, and R. A. Simha, *Rev. Mod. Phys.* **85**, 1143 (2013).
- [9] S. J. Ebbens and J. R. Howse, *Soft Matter* **6**, 726 (2010).
- [10] M. Lighthill, *Communications on pure and applied mathematics* **5**, 109 (1952).
- [11] H. Brenner, *Chem. Engg. Sci.* **18**, 1 (1963).
- [12] B. A. Finlayson and L. E. Scriven, *Proc. Roy. Soc. A* **310**, 183 (1969).
- [13] R. Singh and R. Adhikari, *J. Phys. Commun.* **2**, 025025 (2018).
- [14] A. Solovev and B. M. Friedrich, *The European Physical Journal E* **44**, 1 (2021).
- [15] J. M. Crowley, *J. Fluid Mech.* **45**, 151 (1971).
- [16] J. M. Crowley, *Phys. Fluids* **19**, 1296 (1976).
- [17] R. Lahiri and S. Ramaswamy, *Physical review letters* **79**, 1150 (1997).
- [18] D. R. Brumley and T. J. Pedley, *Phys. Rev. Fluids* **4**, 053102 (2019).
- [19] R. Chajwa, N. Menon, S. Ramaswamy, and R. Govindarajan, *Physical Review X* **10**, 041016 (2020).
- [20] R. I. McLachlan, *Phys. Rev. Lett.* **71**, 3043 (1993).
- [21] R. I. McLachlan, G. R. W. Quispel, and N. Robidoux, *Phys. Rev. Lett.* **81**, 2399 (1998).
- [22] P. J. Olver, *Applications of Lie groups to differential equations*, Vol. 107 (Springer Science & Business Media, 2000).
- [23] J. E. Marsden and T. S. Ratiu, *Introduction to mechanics and symmetry: a basic exposition of classical mechanical systems*, Vol. 17 (Springer Science & Business Media, 2013).
- [24] H. Goldstein, *Classical mechanics* (Addison-Wesley, 1980).
- [25] V. I. Arnold, *Mathematical methods of classical mechanics*, Vol. 60 (Springer, New York, 2013).
- [26] L. M. Hocking, *Journal of Fluid Mechanics* **20** (1964), 10.1017/S0022112064001070.
- [27] A. Zöttl and H. Stark, *Phys. Rev. Lett.* **108**, 218104 (2012).
- [28] A. Zöttl and H. Stark, *The European Physical Journal E* **36**, 1 (2013).
- [29] E. Lushi and P. M. Vlahovska, *Journal of Nonlinear Science* **25**, 1111 (2015).
- [30] H. Stark, *The European Physical Journal Special Topics* **225**, 2369 (2016).
- [31] Q. Brosseau, F. B. Usabiaga, E. Lushi, Y. Wu, L. Ristroph, J. Zhang, M. Ward, and M. J. Shelley, *Phys. Rev. Lett.* **123**, 178004 (2019).
- [32] P. Tallapragada and S. Sudarsanam, *Physical Review E* **100**, 062207 (2019).
- [33] R. Chajwa, N. Menon, and S. Ramaswamy, *Physical Review Letters* **122**, 224501 (2019).
- [34] A. Bolitho, R. Singh, and R. Adhikari, *Phys. Rev. Lett.* **124**, 088003 (2020).
- [35] B. M. Mognetti, A. Šarić, S. Angioletti-Uberti, A. Cacciuto, C. Valeriani, and D. Frenkel, *Phys. Rev. Lett.* **111**, 245702 (2013).
- [36] S. Herminghaus, C. C. Maass, C. Krüger, S. Thutupalli, L. Goehring, and C. Bahr, *Soft Matter* **10**, 7008 (2014).
- [37] C. C. Maass, C. Krüger, S. Herminghaus, and C. Bahr, *Annual Review of Condensed Matter Physics* **7**, 171 (2016).
- [38] C. Krüger, C. Bahr, S. Herminghaus, and C. C. Maass, *The European Physical Journal E* **39**, 64 (2016).
- [39] R. Seemann, J.-B. Fleury, and C. C. Maass, *The European Physical Journal Special Topics* **225**, 2227 (2016).
- [40] A. Caciagli, R. Singh, D. Joshi, R. Adhikari, and E. Eiser, *Physical Review Letters* **125**, 068001 (2020).
- [41] R. Singh, *Microhydrodynamics of active colloids [HBNI Th131]*, Ph.D. thesis, HBNI (2018).
- [42] S. Kim and S. J. Karrila, *Microhydrodynamics: Principles and Selected Applications* (Butterworth-Heinemann, Boston, 1991).
- [43] H. Faxén, *Ann. der Physik* **373**, 89 (1922).
- [44] B. Felderhof, *Physical Review E* **68**, 051402 (2003).
- [45] F. Estabrook and H. Wahlquist, *Siam Review* **17**, 201 (1975).
- [46] R. Singh and R. Adhikari, *Phys. Rev. Lett.* **117**, 228002 (2016).
- [47] S. Thutupalli, D. Geyer, R. Singh, R. Adhikari, and H. A. Stone, *Proc. Natl. Acad. Sci.* **115**, 5403 (2018).
- [48] A. Bolitho and R. Adhikari, In preparation.
- [49] E. Campbell, *Journal of Physics and Chemistry of Solids* **24**, 197 (1963).
- [50] J. M. Borwein, M. Glasser, R. McPhedran, J. Wan, and I. Zucker, *Lattice sums then and now*, 150 (Cambridge University Press, 2013).
-

Appendix A: Lattice sums in one dimension

The Greens function of an unbounded viscous medium \mathbf{G} given by

$$\mathbf{G}(\mathbf{R}_i, \mathbf{R}_j) = \frac{1}{8\pi\eta r} (\mathbf{I} + \hat{\mathbf{r}}_{ij} \hat{\mathbf{r}}_{ij}) \quad (\text{A1})$$

where $\mathbf{r}_{ij} = \mathbf{R}_i - \mathbf{R}_j$ and $\hat{\mathbf{r}}_{ij} = \mathbf{r}_{ij}/r_{ij}$ which may also be written as

$$\mathbf{G}(\mathbf{R}_i, \mathbf{R}_j) = (\nabla^2 \mathbf{I} - \nabla \nabla) r_{ij} \quad (\text{A2})$$

The lattice sums required to calculate the hydrodynamical interactions of the one-dimensional chain can be evaluated using

$$\begin{aligned} \sum_l \left[\frac{\partial \boldsymbol{\mu}_{il}^{TT}}{\partial \mathbf{R}_j} \cdot m\mathbf{g} \right]_* &= \sum_l \left[\frac{\partial}{\partial \mathbf{R}_j} \frac{1}{8\pi\eta r_{il}} (m\mathbf{g} + \hat{\mathbf{r}}_{il} (\hat{\mathbf{r}}_{il} \cdot m\mathbf{g})) \right]_* \\ &= -\frac{mg}{8\pi\eta r_{ij}^2} [-(\hat{\mathbf{z}} + \hat{\mathbf{r}}_{ij} (\hat{\mathbf{r}}_{ij} \cdot \hat{\mathbf{z}})) \hat{\mathbf{r}}_{ij} + \mathbf{I} (\hat{\mathbf{r}}_{ij} \cdot \hat{\mathbf{z}}) + \hat{\mathbf{r}}_{ij} \hat{\mathbf{z}}]_* \\ &= \frac{mg}{8\pi\eta r_{ij}^2} [\hat{\mathbf{z}} \hat{\mathbf{r}}_{ij} - \hat{\mathbf{r}}_{ij} \hat{\mathbf{z}}] \end{aligned} \quad (\text{A3})$$

where, by parity, $\sum_l \hat{\mathbf{r}}_{jl} = 0$. Using a similar procedure and setting $\mathbf{r}_{ij}^* = \mathbf{R}_i^* - \mathbf{R}_j^* = na\hat{\mathbf{x}}$, the following lattice sums can then be evaluated:

$$\sum_{ln} e^{ikna} \left[\frac{\partial \boldsymbol{\mu}_{il}^{TT}}{\partial \mathbf{R}_j} \cdot m\mathbf{g} \right]_* = \frac{img}{4\pi\eta a^2} (\hat{\mathbf{z}} \hat{\mathbf{x}} - \hat{\mathbf{x}} \hat{\mathbf{z}}) \sum_{n=1}^{\infty} \frac{\sin nka}{n^2} \quad (\text{A4})$$

$$\sum_{ln} e^{ikna} \left[\hat{\mathbf{z}} \times \frac{\partial \boldsymbol{\mu}_{il}^{RT}}{\partial \mathbf{R}_j} \cdot m\mathbf{g} \right]_* = \frac{mg}{4\pi\eta a^3} (\mathbf{I} - \hat{\mathbf{z}} \hat{\mathbf{z}} - 3\hat{\mathbf{x}} \hat{\mathbf{x}}) \sum_{n=1}^{\infty} \left(\frac{\cos nka}{n^3} - \frac{1}{n^3} \right) \quad (\text{A5})$$

Appendix B: Lattice sums in two dimensions

Taking the lattice to be rectangular with $\mathbf{r}_{ij} = na\hat{\mathbf{x}} + ma\hat{\mathbf{y}}$, the two-dimensional lattice sums required are then

$$\sum_{lnm} e^{i(k_1 n + k_2 m)a} \left[\frac{\partial \boldsymbol{\mu}_{il}^{TT}}{\partial \mathbf{R}_j} \cdot m\mathbf{g} \right]_* = \frac{img}{4\pi\eta a^2} \sum_{nm} [\hat{\mathbf{z}} \hat{\mathbf{r}}_{ij} - \hat{\mathbf{r}}_{ij} \hat{\mathbf{z}}]_* \frac{\sin(nk_1 + mk_2)a}{n^2 + m^2} = -\frac{ia}{\lambda} (\hat{\mathbf{z}} \mathbf{s}(\mathbf{k}) - \mathbf{s}(\mathbf{k}) \hat{\mathbf{z}}), \quad (\text{B1})$$

$$\sum_{lnm} e^{i(k_1 n + k_2 m)a} \left[\hat{\mathbf{z}} \times \frac{\partial \boldsymbol{\mu}_{il}^{RT}}{\partial \mathbf{R}_j} \cdot m\mathbf{g} \right]_* = \frac{mg}{4\pi\eta a^3} \sum_{nm} [\mathbf{I} - \hat{\mathbf{z}} \hat{\mathbf{z}} - 3\hat{\mathbf{r}}_{ij} \hat{\mathbf{r}}_{ij}]_* \frac{\cos(nk_1 + mk_2)a - 1}{(n^2 + m^2)^{3/2}} = \frac{a^2}{\lambda b} c(\mathbf{k}) (\mathbf{I} - \hat{\mathbf{z}} \hat{\mathbf{z}} - 3\hat{\mathbf{k}} \hat{\mathbf{k}}), \quad (\text{B2})$$

where \sum_{nm}^{∞} implies summation over all lattice points $n > 0, -\infty < m < \infty$ in the half-plane Γ and $\hat{\mathbf{r}}_{ij} = (n, m)/\sqrt{n^2 + m^2}$. These sums are conditionally convergent [49, 50] yielding finite expressions for $\mathbf{s}(\mathbf{k}), c(\mathbf{k})$. In particular, the sum

$$\mathbf{s}(\mathbf{k}) = \sum_{nm}^{\infty} \hat{\mathbf{r}}_{ij} \frac{\sin(nk_1 + mk_2)a}{n^2 + m^2} = s(\mathbf{k}) \hat{\mathbf{k}} \quad (\text{B3})$$

since $\sin(\mathbf{k} \cdot \hat{\mathbf{r}}_{ij}) = 0$ when $\hat{\mathbf{r}}_{ij} \perp \mathbf{k}$ and therefore only components parallel to the wavevector contribute when the sum is taken over all lattice points.